Effects of Gaps Among Panels in Radio Astronomy Reflector Antennas

Giuseppe Pelosi, Roberto Coccioli, Alessio Gaggelli

Abstract— **The main reflector of antennas used for radio astronomy consists of hundreds of panels among which, for various reasons, small gaps are left. In this paper, the effects of these gaps on the field scattered by the reflector are analyzed by means of an hybrid numerical technique which combines the Finite Element Method (FEM) and the Method of Moments (MoM). Numerical results pertaining to the case of an incident plane wave are presented, and the effects of the introduction of corrugations inside the gaps to minimize the power flowing through the gaps themselves are discussed.**

I. Introduction

THE construction of the main reflector is the most difficult mechanical problem encountered in the realization of both radio telescope and large antennas such as those used for telecommunications in deep space. The main reflector is realized as a collection of conductive panels whose shapes are usually trapezoidal or hexagonal. The panels are left separated by a small gap to account for thermal expansion, deformations due to gravity, and to ease the construction of the reflector itself. For radio astronomy applications, the main issues are the antenna maneuverability (from a mechanical point of view) and the antenna gain over a wide frequency band (from an electromagnetic point of view).

The reflector for these antennas is usually designed assuming its surface as smoothly curved and continuous and using high frequency techniques. This approach is most useful, but unfortunately it is not able to account for the presence of gaps whose effects in the antenna performance are usually neglected [1]. More flexible and accurate numerical methods, such as the Finite Element Method (FEM) [2]-[3], can be used to simulate the presence of the gaps. Electromagnetic scattering from gaps in perfectly conducting planes has been analyzed by Gedney and Mittra [4] and Jin and Volakis [5] using a hybrid FEM/Method of Moments and FE/Boundary Integral technique, respectively. The aim of this work is to extend the numerical analysis to the practical problem of gaps among tilted metallic planes as it is the case in reflector antennas.

G. Pelosi, R. Coccioli and A. Gaggelli are with the Microwave Laboratory, Department of Electrical Engineering, University of Florence, Via C. Lombroso 6/17, I-50134 Florence, Italy.

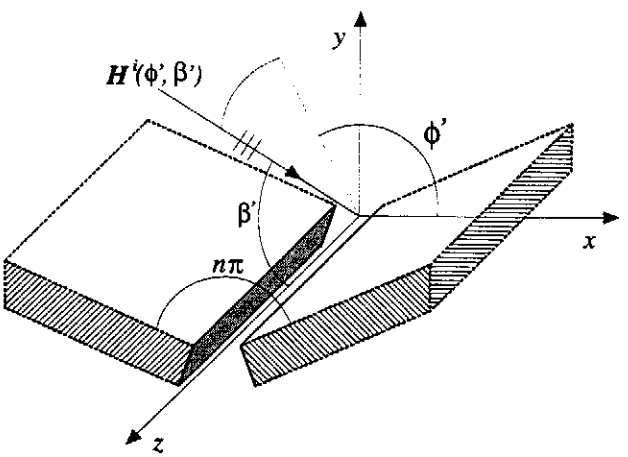

Fig. 1. Geometrical model of a gap between two tilted panels.

To develop an efficient analysis tool, the hybrid technique proposed in [6] to analyze electromagnetic scattering from a wedge with cavity-backed apertures in its faces, is modified and applied to this case. Resorting to this hybrid method limits the applications of the FEM to the gap, while using high frequency techniques to simulate the large reflector. Moreover, the flexibility of the FEM allows considering the actual geometric configuration of the problem, in which the angle formed by two panels of the main reflector varies according to their location in the reflector itself, or the panels present corrugation in their edges to reduce transmission through the gap [7].

The hybrid technique employed relies on a particular formulation of the equivalence principle which implies covering the gap apertures with metallic plates. The original configuration is thus subdivided into two exterior problems, each of which is comprised of a perfectly conducting wedge, and an interior problem, consisting of a cavity with the same shape as

the gap. The exterior canonical problems are formulated by exploiting the exact perfectly conducting wedge Green's function, while the more involved interior problem is treated by means of the FEM. The solutions are then joined by enforcing the continuity condition of the fields at each gap aperture. This procedure restricts the application of the FEM to the small geometric domain constituted by the gap. Furthermore, using the Finite Element Method to analyze the interior problem allows treating odd shaped gaps, such as those existing between tilted panels, which cannot be easily taken into account with other numerical techniques.

The hybrid technique employed is briefly outlined in Section II. The numerical solution implemented is described in Section III. Finally, numerical results are presented in Section IV to demonstrate both the accuracy of the technique and the effects of the gaps.

II. Formulation

Since the wavelength is always much smaller than the panel dimensions, the reflector surface can be locally approximated by a geometric canonical model constituted by two half-planes of finite thickness forming an angle $n\pi$ (Fig. 1). This canonical model is assumed as uniform along the z-axis, which is parallel to the half-plane edges, while ϕ' and β' denote the direction of propagation of the incident field. The following analysis has been carried out by considering the case $\beta' = \pi/2$ and an incident plane wave with unitary magnetic field parallel to the z-axis (TE_z case, $E_z^{inc} = 0$). Since the evaluation of power losses due to transmission of the field through the gap is the parameter of interest, only this polarization needs to be considered. In fact, since the width of the gap is much smaller than the wavelength over the frequency range of interest, TM_z waves do not propagate through the gap. The time dependence $\exp(j\omega t)$ has been assumed and suppressed in the following analysis.

The procedure proposed in this paper, which is an extension of that presented in [6], consists of two consecutive steps. In the first step, two fictitious surfaces Γ_1 and Γ_2 are defined by extending in free space the faces of the perfectly conducting panels, so that they intersect at Q and Q' respectively (Fig. 2). Then, the equivalence theorem is applied so as to subdivide the problem into three separate configurations (Fig. 3), simpler than the original one. Accordingly, the surfaces Γ_1 and Γ_2 are closed with a perfectly conducting cover and the three new problems are coupled through the equivalent surface magnetic current densities $\mathbf{M}^{ext1,2}$ and $\mathbf{M}^{int1,2}$, which are impressed on opposite sides of the

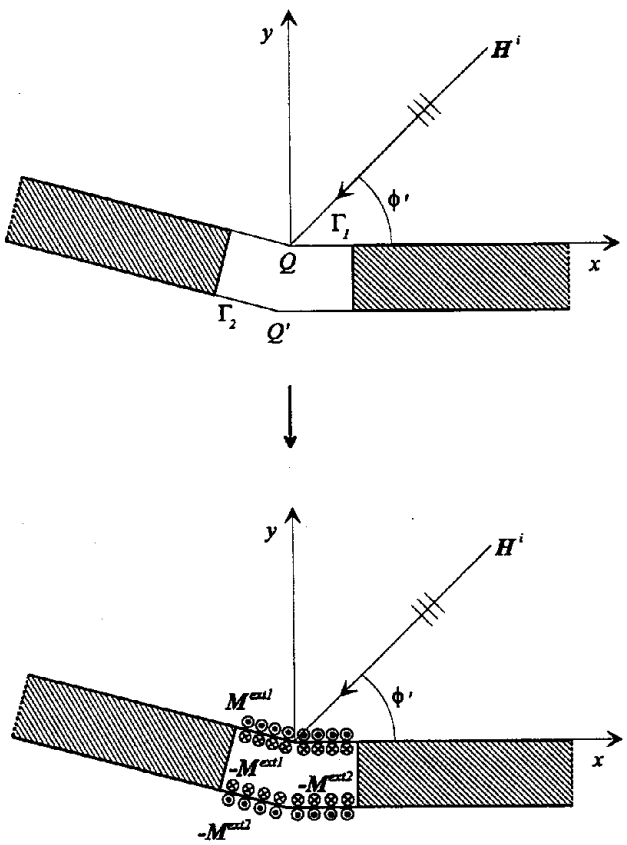

Fig. 2. Surfaces Γ_1 and Γ_2 used for the application of the equivalence principle.

surfaces $\Gamma_{1,2}$. Consequently, the original problem is reduced to: *i*) the analysis of the field in the exterior region of two complementary perfectly conducting wedges (Fig. 3a); *ii*) the analysis of the field inside the equivalent closed cavity (Fig. 3b).

For case *i*), the first exterior problem refers to the front part of the reflector and it is necessary to compute the magnetic field due to the incident plane wave and the unknown exterior magnetic current $\mathbf{M}^{ext1}$ at Γ_1 (Fig. 3a), defined as $\mathbf{M}^{ext1} = \mathbf{E}\times\hat{\mathbf{n}}$, where $\hat{\mathbf{n}}$ is the outward normal unit vector to Γ_1 and $\mathbf{E}$ is the electric field at the same surface. The second exterior problem, similar to the previous one except for the absence of excitation from the backside of the reflector, consists of the evaluation of the field radiated by the equivalent currents $\mathbf{M}^{ext2} = \mathbf{E}\times\hat{\mathbf{n}}$. These latter radiate in the presence of the reconstructed perfectly conducting wedge with its edge in Q' (Fig. 3a). Solution of the problem *ii*) implies the computation of the field radiated by the unknown magnetic currents $\mathbf{M}^{int1,2}$ inside the equivalent closed cavity sketched in Fig. 3b.

The second step of the procedure consists of

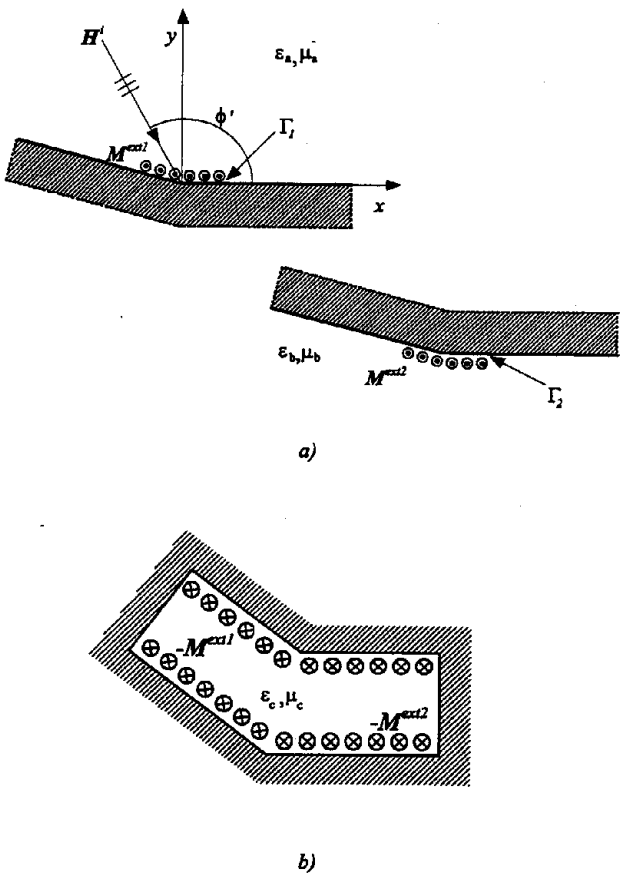

Fig. 3. *a)* Exterior problems. *b)* Interior problem. The three problems are coupled through the equivalent magnetic currents.

matching the exterior and interior problems. This can be achieved by enforcing the continuity, across the surfaces $\Gamma_{1,2}$, of the tangential component of the total electric and magnetic fields. By choosing the interior current as $\mathbf{M}^{int1,2} = -\mathbf{M}^{ext1,2}$, the continuity of the tangential component of the electric field is automatically guaranteed, while the boundary condition on the magnetic field must be explicitly enforced:

$$\hat{\mathbf{n}} \times \mathbf{H}^{ext1} = \hat{\mathbf{n}} \times \mathbf{H}^{int1}, \quad (1a)$$

$$\hat{\mathbf{n}} \times \mathbf{H}^{ext2} = \hat{\mathbf{n}} \times \mathbf{H}^{int2}. \quad (1b)$$

Regardless of the matching procedure adopted, the exterior magnetic field $\mathbf{H}^{ext1} = \hat{\mathbf{z}} H_z^{ext1}$ in equation (1a), which is defined in problem i), may be expressed as the superposition of three contributions:

$$H_z^{ext1} = H_z^{inc} + H_z^{scat} + H_z^{rad1}(\mathbf{M}^{ext1}), \quad (2)$$

where H_z^{inc} is the incident field, H_z^{scat} is the field scattered by the equivalent wedge and $H_z^{rad1}(\mathbf{M}^{ext1})$ is the field radiated by the exterior equivalent surface currents impressed on Γ_1. In the second exterior problem just one term is present, that is the $H_z^{ext2} = H_z^{rad2}(\mathbf{M}^{ext2})$. The scattered field H_z^{scat} is evaluated by using the perfectly conducting wedge Green's function expressed in terms of eigenfunctions [8], or its Uniform Geometrical Theory of Diffraction (UTD) approximation [9], depending on the distance between the observation point and the edge Q of the equivalent wedge. The evaluation of the contribution $H_z^{rad1,2}(\mathbf{M}^{ext1,2})$, due to the equivalent magnetic current distribution, has been done only with perfectly conducting wedge Green's function because the surfaces $\Gamma_{1,2}$ are always close to the edge of the wedge. The interior magnetic field $\mathbf{H}^{int1,2} = \hat{\mathbf{z}} H_z^{int1,2}$ in the right hand side of equations (1a) and (1b) is produced by the interior equivalent surface current distribution impressed on $\Gamma_{1,2}$: $H_z^{int1,2} = H_z^{int1,2}(\mathbf{M}^{int1}, \mathbf{M}^{int2}) = H_z^{int1,2}(-\mathbf{M}^{ext1}, -\mathbf{M}^{ext2})$ and it is computed via the FEM solving the scalar Helmholtz equation for this field component.

Two different matching techniques, belonging to the inward-looking and outward-looking [10] categories, could be employed. Since the gaps among panels have dimensions much smaller than the wavelength in the frequency range of interest, the continuity condition in equations (1a) and (1b) can be directly solved by a point-matching formulation of the MoM, as suggested in [11]. The use of this scheme makes it necessary to explicitly calculate the contribution arising from the interior problem to the impedance matrix of the MoM. To this end, the FEM is employed to evaluate the magnetic field on $\Gamma_{1,2}$, due to each basis function used to expand the interior magnetic current distribution $\mathbf{M}^{int1,2} = -\mathbf{M}^{ext1,2}$ on $\Gamma_{1,2}$ itself. This procedure belongs to the inward-looking formulation class, and similarly to all the procedures of this kind, it is numerically efficient. As a matter of fact, it first solves the interior problem, which requires the inversion of a sparse, symmetric, and real (for lossless materials filling the cavity) matrix, and afterwards it matches the interior and the exterior problem. This latter task requires the solution of a system of equations whose coefficient matrix is full, but smaller than that related to the interior problem.

This matching scheme also retains the major shortcoming of inward-looking formulations: it suffers from the possible presence of non-physical resonant solutions, which may arise when solving the closed interior problem in the lossless case. However, due to the dimensions of the interior problem, this is not an issue in this application.

III. Numerical Implementation

The inward-looking formulation for the problem leads to the standard MoM matrix equation

$$[\mathbf{Y}^{int1} + \mathbf{Y}^{ext1} + \mathbf{Y}^{int2} + \mathbf{Y}^{ext2}] \cdot \mathbf{V} = \mathbf{I}, \qquad (3)$$

where $\mathbf{Y}^{int1,2}$ and $\mathbf{Y}^{ext1,2}$ account for the contributions to the magnetic field at $\Gamma_{1,2}$ coming from the interior and the exterior problem, respectively. Furthermore, in equation (3), $\mathbf{I}$ is the excitation column vector, due to the incident plus scattered fields at the aperture opening Γ_1, while $\mathbf{V}$ is the column vector of the unknown coefficients of the basis functions used to expand the equivalent magnetic current distribution. Careful attention must be paid in choosing this set of basis functions. As a matter of fact, the transverse components of the electric field are singular [12], [13] at the two edges of each of the thick panels delimiting the gap and this singularity is apparently also present in the equivalent magnetic current. For this reason, the four basis functions centered at the ends of the fictitious surfaces Γ_1 and Γ_2 have been chosen with a singular behavior of the kind $-1/(2\sqrt[3]{\rho})$, where ρ is the distance from the edge of the wedge. Indeed, this is the kind of singularity that the transverse component of the electric field exhibits at the proximity of a 90° perfectly conducting wedge [13]. These four basis functions, as well as all the other, span a subsection of Γ_1 and Γ_2 and are built in such a way that they vanish at all the other nodal points on Γ_1 and Γ_2 belonging to the same subsection. All the other basis functions are polynomials which, on the surfaces Γ_1 or Γ_2, coincide with the shape functions used for the FEM discretization of the interior problem.

The magnetic field required to calculate each entry of the matrix $\mathbf{Y}^{int1,2}$ is obtained by applying the finite element method with second order nodal elements to the interior region. The FEM has been chosen because it allows rather general equivalent cavity configurations, such as those arising in case of arbitrarily tilted panels, corrugations in the thick side of the panels, the presence of dielectric material, and so on. It is important to remark that the construction of this $(N \times N)$ matrix, which needs the solution of N interior problems (where N is the number of basis functions used to expand all the magnetic equivalent currents on Γ_1 and Γ_2), can be done just once for each gap configuration, regardless the direction of the incident wave.

$\mathbf{Y}^{ext1,2}$ in equation (3) results from the term $\mathbf{H}_z^{rad1,2}(\mathbf{M}^{ext1,2})$, and is evaluated by referring to the equivalent problem of a wedge illuminated by a magnetic line source. Also the construction of this matrix can be done just once for a gap with a specified aperture, and subsequently used for any direction of the incident electromagnetic field.

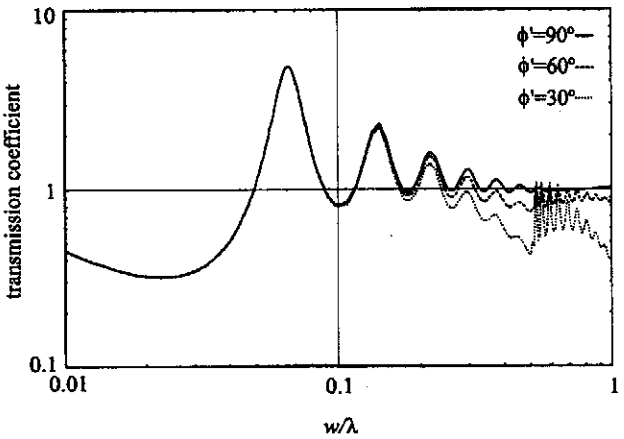

Fig. 4. Transmission coefficient through a 0.05 cm wide gap in a 0.3 cm thick conducting panel for different angles of incidence.

IV. Numerical Results

To validate the code, previously published results and measurements have been considered. Fig. 4 shows the transmission coefficient through a slot with width $w = 0.05$ cm in a 0.3 cm thick conducting sheet. Computations have been performed for three different values of the incidence angle, and results agree very well with those reported in [4]. It should be noted that the transmission coefficient has been defined as the ratio between the power flowing through the gap and that through the same surface located in the free space due to a plane wave impinging at $\phi' = 90°$, and this accounts for the values above unity in Fig. 4.

A second comparison has been made analyzing a more involved configuration, for which measured results are available in the literature [14]. It is comprised of a gap with length 3.6 mm between two perfectly conducting panels 5 mm thick. Each panel has a corrugation 3 mm wide and 7.5 mm deep. Fig. 5 shows, for a such configuration, the transmission coefficient versus frequency, where the transmission coefficient is defined as the ratio of the power flowing through the gap with the corrugation and without. When the panels are aligned ($n = 1$), the measured transmission coefficient from reference [14] (dots) agrees well with the computed one (dashed line). It can be seen that, at a frequency close to the resonant frequency of the corrugations, the transmission coefficient becomes quite low, increasing the antenna performance. Fig. 5 also shows the transmis-

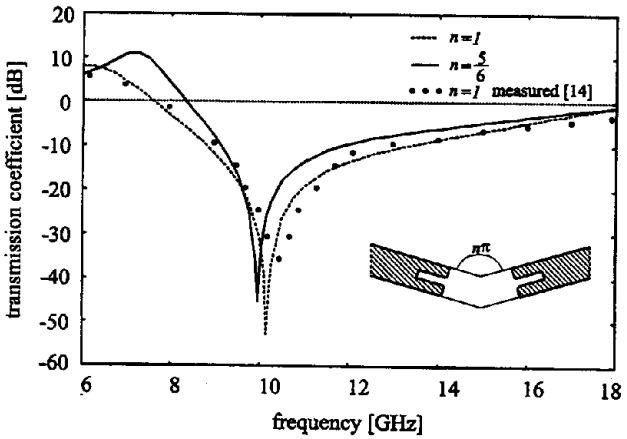

Fig. 5. Transmission coefficient through a slit between two panels 5 mm thick. Each panel presents a corrugation 7.5 mm deep and 3 mm wide. $\phi' = 75°$. Dashed line: $n = 1$, computed results; dots: $n = 1$, measured results [14]; continuous line: $n = 5/6$, computed results.

sion coefficient versus frequency when the two panels are tilted of an angle equal to 150° ($n = 5/6$, continuous line). The length of the gap Γ_1 is kept constant to 3.6 mm, but since the opposite faces of the panels are moved farther from each other, the resonance frequency of the corrugated gap decrease, as shown by the computed results.

Fig. 6 shows the amplitude of the magnetic field longitudinal component H_z inside the gap relative to the case $n = 5/6$ of Fig. 5. The incident field has a frequency of 10 GHz and for such value the corrugation depth is equal to $\lambda/4$. Hence, the corrugations create an equivalent magnetic wall along the thick side of the panels, which act as a short circuit on the magnetic field. As matter of fact, Fig. 6 shows maxima of magnetic field at the end of the corrugations and minima at their entrance. The low level of the magnetic field at the surface Γ_2 accounts for the minimum in the transmission coefficient through the aperture. Although introducing the corrugation is effective only in a narrow band, and thus it is not possible to optimize the radio astronomy reflector antenna performance in the whole frequency band of interest, corrugations may be used to optimize the antenna in specific relatively narrow bands as, for instance, those also used for telecommunication purposes.

The third configuration considered is comprised of a 6 mm wide gap between 2 mm thick panels tilted at an angle of 170°. These parameters have been measured directly on the parabolic radio astronomy reflector antenna of the Italian National Research Council located at Medicina (Bologna, Italy).

In Fig. 7, the equivalent magnetic currents at the

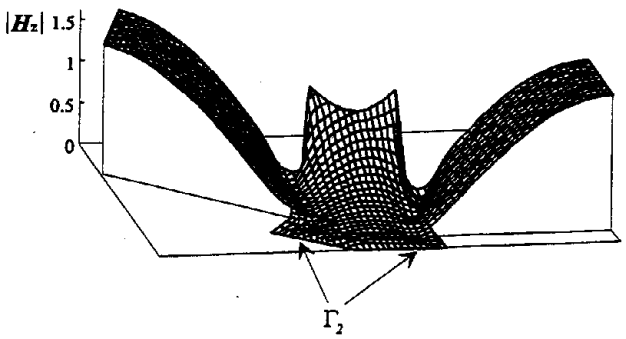

Fig. 6. Amplitude of the magnetic field longitudinal component inside a corrugated gap between two panels 5 mm thick and tilted at 150°. Each panel presents a corrugation 7.5 mm deep and 3 mm wide. $\phi' = 75°$, $f = 10$ GHz.

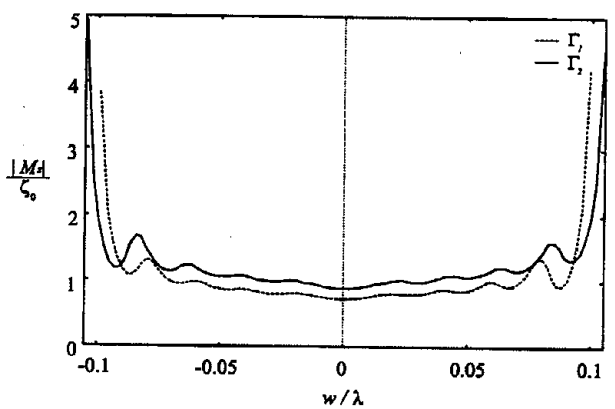

Fig. 7. Normalized amplitude of equivalent magnetic current distributions at surfaces Γ_1 and Γ_2 for a slit 6 mm wide and 2 mm deep between two panels tilted at 170°. The incident plane wave impinges at an angle $\phi' = 85°$ and has a frequency equal to 10 GHz.

apertures Γ_1 and Γ_2 are plotted. The incident plane wave has a frequency equal to 10 GHz and impinges at an angle of $\phi' = 85°$. At both the apertures, the equivalent current distribution is almost uniform in the central part, while it exhibits the expected singularity near the edges of the panels. These equivalent magnetic currents provide an almost isotropic radiation pattern. This means that radiation incoming from the backside of the reflector is received through the gap, thus increasing the antenna noise temperature.

Further interesting results pertains to the field scattered by the two panels. Fig. 8 shows the normalized amplitude of the scattered field at a distance of $\rho = 10\lambda$ from the reconstructed wedge Q versus the observation angle. The two panels are illuminated by a plane wave impinging again at $\phi' = 85°$ but with a frequency equal to 50 GHz. The dotted

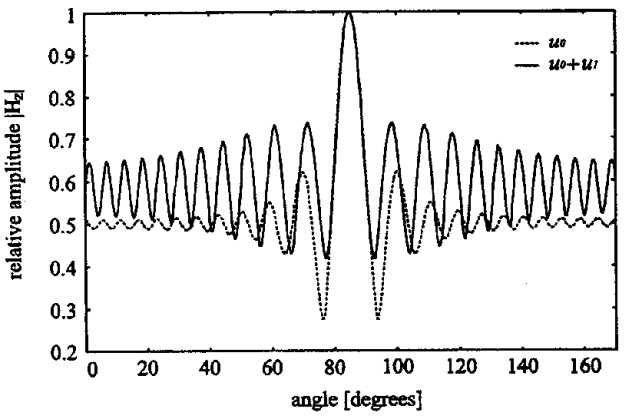

Fig. 8. Normalized amplitude of the magnetic field at a distance $\rho = 10\lambda$ from the reconstructed wedge Q of two panels tilted at 170°. $\phi' = 85°$; $f = 50$ GHz. Dots: continuous panels, the presence of the gap is neglected. Continuous line: the presence of a slit 6 mm wide and 2 mm deep is considered.

line refers to the field computed by neglecting the presence of the gap. This field, denoted as u_0, represents a zero-th order solution. The first order additive contribution u_1 is given by the field radiated by the equivalent magnetic current computed with the technique proposed. The field $u_0 + u_1$ is shown in Fig. 8 with a continuous line. It is seen that in the backscattering direction there are no differences between the two patterns, while the contribution u_1 of the gap strongly affects the radiation pattern in the other directions, and this effect increases with frequency.

V. Conclusion

The effects of gaps among panels comprising the main reflector of large antennas used for radio astronomy have been studied by means of a hybrid numerical technique which combines the FEM and the MoM. The technique is based on a particular application of the equivalence principle which allows the reduction of the original configuration to three simpler problems: two exterior canonical problems and one interior problem. The first two can be treated by exploiting the exact Green's function or its approximation in the framework of the Uniform Geometrical Theory of Diffraction, the latter can be efficiently solved using the FEM. Due to the flexibility of the FEM, it is possible to analyze arbitrary configurations in an attempt to find optimized gap configurations able to improve the antenna performance.

The code realized in this work represents a first step toward a more sophisticated tools able to evaluate the contribution to the phase error at the antenna opening due to the presence of gaps between panels. This contribution, as shown by the results presented, may be significant.

Acknowledgment

The authors wish to thank Dr. E. Paoletti of the University of Florence for useful discussions and help with computations.

References

[1] G. Cortés Medellín, P. F. Goldsmith, "Analysis of active surface reflector antenna for a large millimeter wave radio telescope," *IEEE Trans. Antennas Propagat.*, vol. 42, no. 2, pp. 176–183, 1994.

[2] P.P. Silvester, G. Pelosi, *Finite Elements for Wave Electromagnetics.* IEEE Press, New York, 1994.

[3] P. P. Silvester, R.L. Ferrari, *Finite elements for electrical engineers.* 3rd edition. Cambridge, U.K.: Cambridge University Press, Cambridge, 1996.

[4] S. D. Gedney, R. Mittra, "Electromagnetic transmission through inhomogeneously filled slots in a thick conducting plane - arbitrary incidence," *IEEE Trans. Electromagn. Compat.*, vol. 34, no. 4, pp. 404–415, 1992.

[5] J. M. Jin, J. L. Volakis, "Electromagnetic scattering by and transmission through a three-dimensional slot in a thick conducting plane," *IEEE Trans. Antennas Propagat.*, vol. 39, no. 4, pp. 543–550, 1991.

[6] G. Pelosi, R. Coccioli, G. Manara, A. Monorchio, "Scattering from a wedge with cavity backed aperture in its faces and related configurations: TE case," *IEE Proc.-Microw. Antennas Propagat.*, vol. 142, no. 2, pp. 183–188, April 1995.

[7] P. S. Kildal, L. Steen, P. Napier, "Reduction of scattering from gaps between reflector antennas panels by using artificially soft edges," *Antennas and Propagation Society Symposium 1991 Digest*, London, Ont., Canada, 24-28 June 1991, vol. 3, pp. 1316–1319, 1991.

[8] R. F. Harrington, *Time Harmonic Electromagnetic Fields.* McGraw-Hill, New York, 1961.

[9] R. G. Kouyoumjian, P. H. Pathak, "A uniform geometrical theory of diffraction for an edge in a perfectly conducting surface," *Proc. IEEE*, vol. 62, pp. 1448–1461, 1974.

[10] L. W. Pearson, A. F. Peterson, L. J. Bahrmasel, R. A. Whitaker, "Inward-looking and outward-looking formulations for scattering from penetrable objects," *IEEE Trans. Antennas Propagat.*, vol. 40, no. 6, pp. 714–720, 1992.

[11] X. Yuan, D. R. Lynch, J. W. Strohbehn, "Coupling of finite element and moment methods for electromagnetics scattering from inhomogeneous objects," *IEEE Trans. Antennas Propagat.*, vol. 38, no. 3 pp. 386–393, 1990.

[12] J. Meixner, "The behavior of electromagnetic fields at edges," *IEEE Trans. Antennas Propagat.*, vol. 20, no. 4, pp. 442–446, 1972.

[13] J. Van Bladel, "Field singularities at metal-dielectric metal wedges," *IEEE Trans. Antennas Propagat.*, vol. 33, no. 4, pp. 450–455, 1985.

[14] J. Carlsson, P. S. Kildal, "Transmission through corrugated slots," *IEEE Trans. Electromagn. Compat.*, vol. 37, no. 1, pp. 114–121, 1995.